Effect of pressure on the first-order Raman intensity in semiconductors

C. Trallero-Giner,* K. Kunc,† and K. Syassen
Max-Planck-Institut für Festkörperforschung, Heisenbergstraße 1, D-70569 Stuttgart, Germany
(Received 12 August 2005; revised manuscript received 21 February 2006; published 12 May 2006)

One-phonon Raman scattering in the zinc-blende-type semiconductors under hydrostatic pressure and with excitation energies below the fundamental gap is examined. A microscopic description of the scattering intensities and Raman cross sections for longitudinal and transverse optical phonons is presented in terms of deformation potential and interband allowed Fröhlich interaction. Calculations are compared to the experimental results for ZnTe, i.e., the variation of the integrated Raman intensity with pressure for LO(Γ) and TO(Γ) modes. So as to make possible a comparison with experimental data, the pressure dependence of all parameters entering into the description of the scattering processes had to be taken into account. In particular, the pressure variation of the relevant conduction band states and optical deformation potential were evaluated using the pseudopotential plane-wave method within the local density approximation to the density functional theory. The present theoretical approach can be used to evaluate the Raman scattering intensities and cross sections in other II-VI and III-V compounds under pressure.

DOI: 10.1103/PhysRevB.73.205202 PACS number(s): 71.38.−k, 63.20.Ls, 78.30.Fs

I. INTRODUCTION

Raman scattering has been used extensively to study the effect of pressure on vibrational properties of tetrahedrally coordinated III-V and II-VI semiconductors.[1–4] Most investigations focused on the pressure-induced frequency shifts of zone-center transverse (TO) and longitudinal (LO) optical phonon modes. Changes in Raman line shapes due to phonon-phonon and phonon-electron interactions were addressed in a number of experimental studies (see Refs. 3 and 4 for citations). Further, pressure tuning of the electronic band structure was used to study resonance effects in the Raman scattering intensity at exciting laser energies larger than the fundamental band gap.

Here, we examine what the established theory of Raman scattering predicts[5–10] for the effect of pressure on the first-order Raman scattering intensity under *nonresonant conditions* which in this paper refers to the excitation energy being smaller than the fundamental energy gap. The work is partly motivated by the results of a recent Raman study of ZnTe under pressure.[11] There, the integrated first-order scattering intensities are reported to decrease with increasing pressure.

At ambient pressure, the intensity of first-order Raman scattering has been investigated in detail by changing the exciting laser wavelength in a fixed scattering configuration (see e.g. Ref. 12). Off resonance, the phonon-induced light scattering occurs through the deformation-potential (DP) electron-phonon interaction.[6,9] In case of the longitudinal optical phonon at the Γ point, the interband Fröhlich electro-optical (EO) contribution has to be taken into account.[13] When considering the effect of pressure on the integrated first-order Raman intensities, the two main factors to be considered are the variation of interband excitation energies and the variation of the phonon frequencies.

We employed a microscopic phenomenological model for the Raman intensity of the zinc-blende-type semiconductors described in Refs. 9 and 10, which takes into account all relevant contributions to the first-order scattering processes. As an example, the model is applied to ZnTe. Changes in optical properties, electronic states, phonon vibrations, and electron-phonon interactions induced by external hydrostatic pressure are analyzed, in part with reference to first-principles calculations of the band structure. The influence of these factors on the Raman tensor is examined.

II. FIRST-ORDER RAMAN SCATTERING INTENSITY

For the sake of clarity we summarize in the following the main expressions needed to describe the evolution of the scattering intensity with applied hydrostatic pressure.

A. Basic relations

The scattering intensities for the TO(Γ) or LO(Γ) processes can be expressed as

$$\frac{\partial S}{\partial \Omega} = \frac{1}{V}\int \frac{\partial^2 \sigma}{\partial \Omega\, \partial\, \omega_S} d\omega_S. \tag{1}$$

The Raman cross section for a Stokes process is related to the scattering amplitude W_{FI} by[14]

$$\frac{\partial^2 \sigma}{\partial \Omega\, \partial\, \omega_S} = \frac{V^2}{(2\pi)^2}\frac{\eta_L \eta_S^3}{c^4}\frac{\omega_L \omega_S^3}{(\hbar\, \omega_L)^2}(N_0+1) \times \sum_F |W_{FI}|^2 \delta(\omega_S - \omega_L + \omega_0). \tag{2}$$

Here η_L (η_S) is the refractive index for the incident (scattered) radiation $\omega_L(\omega_S)$, c is the speed of light in vacuum, V is a normalization volume, and N_0 represents the Bose-Einstein distribution function for phonons with frequency ω_0. The electronic system is assumed to be in its ground state in both the initial and final states of the scattering process which are denoted by, respectively, $|I\rangle$ and $|F\rangle$.

The scattering amplitude probability in Eq. (2) can be written as

$$W_{FI} = \sum_{\mu_1,\mu_2} \frac{\langle F|\hat{H}_{E-R}|\mu_2\rangle\langle\mu_2|\hat{H}_{E-L}|\mu_1\rangle\langle\mu_1|\hat{H}_{E-R}|I\rangle}{(\hbar\omega_S - E_{\mu_2})(\hbar\omega_L - E_{\mu_1})} + A. \tag{3}$$

Here $\hat{H}_{E-L}$ and $\hat{H}_{E-R}$ are the Hamiltonians describing the interaction of the electronic system with, respectively, the lattice vibrations and the radiation field, $|\mu_i\rangle$ $(i=1,2)$ is the intermediate electron-hole state with energy E_{μ_i}. Here and throughout the paper, the constant A stands for a dispersionless background coming from other scattering processes;[12] its magnitude may differ depending on spectral range, scattering geometry, and other factors. By permuting the interaction operators in Eq. (3) one obtains other contributions to the Raman cross section Eq. (2) which, however, are small and can be considered to be resumed in the constant A.

Off resonance, the electron-hole correlation (excitons) and the polariton effects are negligible. Hence, the intermediate virtual electronic states $|\mu_i\rangle$ are described by the free electron-hole picture (E-H) at any pressure. In the two-band parabolic model the E-H energy $E_\mu \equiv E(\mathbf{k}_e, \mathbf{k}_h)$ is given by

$$E(\mathbf{k}_e, \mathbf{k}_h) = E_g + \frac{\hbar^2 k_e^2}{2m_e} + \frac{\hbar^2 k_h^2}{2m_h}, \tag{4}$$

where E_g is the fundamental gap, m_e (m_h) and $\mathbf{k}_e$ $(\mathbf{k}_h)$ are the effective mass and wave vector of the electron (hole). The electron-radiation matrix elements in Eq. (3) are given by

$$\langle\mu|\hat{H}_{E-R}|I(F)\rangle = \delta_{\mathbf{k}_e,-\mathbf{k}_h}\frac{e}{m_0}\sqrt{\frac{2\pi\hbar}{\omega_{L(S)}\eta^2_{L(S)}}}\frac{\mathbf{e}_{L(S)}\cdot\mathbf{p}_{cv}}{\sqrt{V}} \tag{5}$$

with $\mathbf{p}_{cv}$ being the interband momentum matrix element between the Γ_{15v} valence and Γ_{1c} conduction bands, $\mathbf{e}_{L(S)}$ the polarization vector of the incident (scattered) light, and m_0 the free-electron mass.

The scattering processes contributing to the first-order Raman cross section, i.e., electron-deformation potential and interband Fröhlich interactions, are shown schematically in Fig. 1. The DP Hamiltonian couples the heavy hole (HH) and light hole (LH) valence bands, while the electro-optical mechanism couples the two upper Γ_{1c} and Γ_{15c} conduction bands.

B. Deformation potential

Assuming two independent HH and LH valence bands v_1 and v_2, and only the Γ_{1c} conduction band of s symmetry, the DP interaction by optical phonons does not couple the Bloch states in the conduction band.[15] Thus, scattering by a phonon with frequency ω_0 and wave vector $\mathbf{q}$ only involves the hole part and the corresponding matrix element in Eq. (3) reduces to[5,9]

$$\langle\mu_2|\hat{H}_{E-L}|\mu_1\rangle = -\delta_{\mathbf{k}'_e,\mathbf{k}_e}\delta_{\mathbf{k}'_h,\mathbf{k}_h+\mathbf{q}}\frac{\bar{u}_0\sqrt{3}}{2a_0}\langle v_2|\hat{D}_h|v_1\rangle \tag{6}$$

with $\bar{u}_0$ being the relative phonon displacement defined by

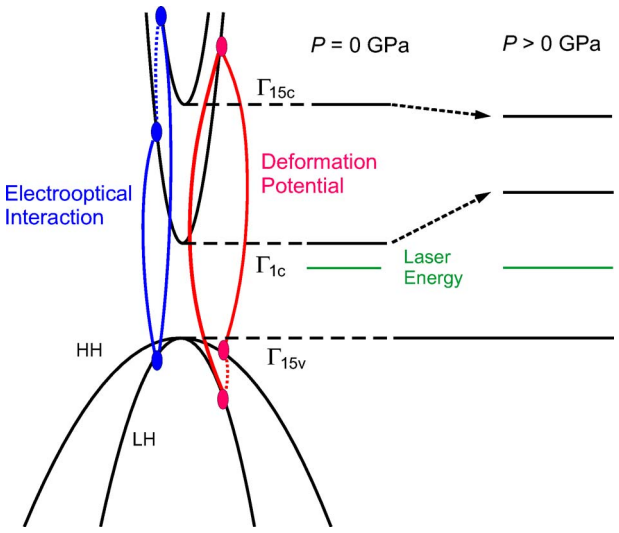

FIG. 1. (Color online) Schematic representation of the deformation potential and interband Fröhlich interactions at the Γ point of the Brillouin zone. The solid lines show the optical transitions and the dashed lines correspond to the electron-phonon-assisted quasiparticle interband transitions. The effect of hydrostatic pressure on the relevant gaps, pertaining to ZnTe, is shown as well.

$$\bar{u}_0 = \left(\frac{\hbar V_c}{2VM^*\omega_0}\right)^{1/2}. \tag{7}$$

Here a_0 is the lattice constant, M^* is the reduced mass of the atoms in the unit cell with volume V_c, and $\langle v_2|\hat{D}_h|v_1\rangle$ is the deformation-potential matrix as defined by Bir and Pikus.[15] Inserting Eqs. (4)–(6) into Eq. (3), after straightforward calculation, the contribution of the DP interaction to the scattering amplitude probability can be written as

$$W^{DP}_{FI} = -\frac{1}{\sqrt{V}}\frac{e^2}{4\sqrt{3}m_0^2}\frac{d_0}{a_0\eta_S\eta_L}\frac{|P_0|^2}{\sqrt{\hbar\omega_L\hbar\omega_S}}\sqrt{\frac{V_c}{M^*\hbar\omega_0}} \times \frac{\sqrt{\mu_{lh}\mu_{hh}}}{\sqrt{E_g - \hbar\omega_S}}\Psi + A \tag{8}$$

with

$$\Psi = F(z) + \frac{1}{\sqrt{z}}F\left(\frac{1}{z}\right)$$

and

$$F(z) = \frac{1}{1 + \sqrt{z\dfrac{E_g - \hbar\omega_L}{E_g - \hbar\omega_S}}}.$$

Here $z=\mu_{hh}/\mu_{lh}$ and μ_{lh} (μ_{hh}) is the electron–light (heavy) hole reduced mass, d_0 is the optical deformation potential, and $P_0=|\langle s|p_x|x\rangle|$.

Inserting Eq. (8) into Eq. (2) one obtains

$$\frac{\partial^2\sigma^{DP}}{\partial\Omega\,\partial\,\omega_S} = C_0|A^{DP}\Psi + A'|^2\frac{(N_0+1)\Gamma}{(\omega_S-\omega_L+\omega_0)^2+\Gamma^2}. \quad (9)$$

Here we have replaced the delta function by a Lorentzian where $1/\Gamma$ is the phonon lifetime. All constants are collected in the factor

$$C_0 = \frac{V}{6(2\pi)^3}\left(\frac{e}{2c\hbar}\right)^4\frac{m_0}{M^*} \quad (10)$$

such that the background amplitude is rescaled accordingly $(A\rightarrow A')$. The deformation potential amplitude factor becomes

$$A^{DP} = -\frac{d_0\omega_S P_0^2}{\omega_L m_0}\sqrt{\frac{\eta_S}{\eta_L}\frac{a_0\mu_{lh}}{\hbar\,\omega_0(E_g-\hbar\,\omega_S)}}\frac{\mu_{hh}}{(m_0)^{3/2}}. \quad (11)$$

This factor contains all the quantities that depend on pressure; the most important are the energy difference $E_g-\hbar\,\omega_S$ and the phonon frequency. At $\hbar\omega_L<E_g$ the other critical points which can couple via DP, e.g., $E_g+\Delta_0$, E_1, and $E_1+\Delta_1$, are very far in energy and their contributions to the scattering amplitude A^{DP} can be resumed in the dispersionless constant A.

C. Interband Fröhlich interaction

In the case of the LO phonon, besides the DP contribution, we have to consider the Fröhlich interaction. For first-order scattering, intraband transitions assisted by LO phonons are forbidden and out of resonance they are negligible. However, the macroscopic electric field can couple two different bands with different symmetry and the Fröhlich mechanism becomes allowed. The interband Fröhlich interaction couples the nearest Γ_{1c} and Γ_{15c} conduction bands (see Fig. 1). In this case the electro-optical (EO) matrix element is given by[5,10]

$$\begin{aligned}\langle\mu_2|\hat{H}_{E-L}|\mu_1\rangle &= \delta_{\mathbf{k}'_e,\mathbf{k}_e+\mathbf{q}}\delta_{\mathbf{k}'_k,\mathbf{k}_h}\frac{C_F}{q\sqrt{V}}\langle u_{c_{15}}|1+i\mathbf{q}\cdot\mathbf{r}|u_{c_1}\rangle \\ &= \delta_{\mathbf{k}'_e,\mathbf{k}_e+\mathbf{q}}\delta_{\mathbf{k}'_k,\mathbf{k}_h}\frac{\hbar}{m_0\sqrt{V}}\frac{C_F}{Ec_{15}-Ec_1}\langle u_{c_{15}}|\mathbf{e}_{LO}\cdot\mathbf{p}|u_{c_1}\rangle, \end{aligned} \quad (12)$$

where $u_{c_{15}}$ and u_{c_1} are the Bloch functions of the Γ_{15c} and Γ_{1c} conduction bands, $\mathbf{e}_{LO}=\mathbf{q}/q$ is the phonon polarization vector, and $Ec_{15}-Ec_1$ is the energy difference between the Γ_{1c} and Γ_{15c} gap energies. The Fröhlich constant C_F is equal to

$$C_F = -i\sqrt{2\pi\hbar\,\omega_{LO}e^2\left(\frac{1}{\varepsilon_\infty}-\frac{1}{\varepsilon_0}\right)} \quad (13)$$

with ε_∞, ε_0, and ω_{LO} being, respectively, the optical and static dielectric constants, and the LO(Γ)-phonon frequency. Combining Eqs. (3), (5), and (12), and assuming, for simplicity, the cross polarization with phonon displacement along the [001] direction, the resulting expression for the EO scattering amplitude probability becomes

$$W_{FI}^{EO} = \frac{|C_F|}{\sqrt{V}}\frac{e^2}{\sqrt{2}m_0^3}\frac{\pi}{a_0\eta_S\eta_L}\frac{QP_0}{\sqrt{\omega_L\omega_S}}\frac{1}{Ec_{15}-Ec_1}\frac{\sqrt{\mu_{lh}}\mu_{hh}}{\sqrt{E_g-\hbar\,\omega_S}}\Phi \quad (14)$$

with

$$\begin{aligned}\Phi = {} & z_{0h}[G(z,Eg;z_{0h},Ec_{15})+G(z_{0h},Ec_{15};z,Eg)] \\ & +\frac{z_{0l}}{3z}[G(1,Eg;z_{0l},Ec_{15})+G(z_{0l},Ec_{15};1,Eg)]\end{aligned}$$

and

$$G(z_1,E_1;z_2,E_2) = \frac{1}{\sqrt{z_1\dfrac{E_1-\hbar\,\omega_L}{E_g-\hbar\,\omega_S}}+\sqrt{z_2\dfrac{E_2-\hbar\,\omega_L}{E_g-\hbar\,\omega_S}}}.$$

Here $iQ=\langle x|p_y|\Gamma_{15c}(z)\rangle$,[16] $z_{0h}(z_{0l})=\mu_{0h}(\mu_{0l})/\mu_{lh}$, and $\mu_{0h}(\mu_{0l})$ denotes the reduced mass between the heavy (light) hole in the valence band and the electron in the Γ_{15c} conduction band. In Eq. (14) the interband matrix element $\langle\Gamma_{15}|p_z|S\rangle=iP'$ of Eq. (12) has been taken equal to $P'=2\pi\hbar/a_0$.[16]

The ratio of the scattering amplitude W^{LO} [Eqs. (8) and (14) for DP and EO contributions by the LO phonon] to W^{TO} [Eq. (8) for DP by TO phonon] determines the Faust-Henry coefficient which gives the strength of the electro-optical mechanism relative to the DP coupling. This coefficient depends on the laser frequency, on the scattering geometry, and also on the applied external pressure. It can be either positive or negative [see Refs. 13 and 17–19]. For the case of ZnTe, treated in the next section, the Faust-Henry coefficient is taken positive as derived in Ref. 20 from the measurements of the absolute Raman efficiency.

The total amplitude for the allowed LO(Γ) scattering is obtained by adding Eqs. (8) and (14), and the corresponding Raman cross section takes the form

$$\frac{\partial^2\sigma^{LO}}{\partial\Omega\,\partial\,\omega_S} = C_0|A^{DP}\Psi + A^{EO}\Phi + A'|^2 \times \frac{(N_{LO}+1)\Gamma_{LO}}{(\omega_S-\omega_L+\omega_{LO})^2+\Gamma_{LO}^2}. \quad (15)$$

With the same constant prefactor C_0 as given in Eq. (10) the amplitude factor A^{EO} becomes

$$A^{EO} = -\,d_0\frac{\omega_S}{\omega_L}|P_0|^2\sqrt{\frac{\eta_S}{\eta_L}\frac{a_0}{\hbar\,\omega_{LO}}}\frac{\sqrt{\mu_{lh}}\mu_{hh}}{\sqrt{E_g-\hbar\,\omega_S}}\alpha. \quad (16)$$

The effective electro-optical constant α introduced above depends on the applied external pressure and is given by

$$\alpha = 4\sqrt{\frac{3\pi}{\varepsilon_\infty}}\pi\frac{e\hbar}{m_0}\frac{\sqrt{(\hbar\omega_{LO})^2-(\hbar\omega_{TO})^2}}{d_0}\frac{Q}{P_0}\frac{\sqrt{\rho}}{Ec_{15}-Ec_1}. \quad (17)$$

ω_{TO} is the TO(Γ) phonon frequency and ρ is the reduced mass density. The important pressure-dependent factors here are the difference between the squared LO and TO frequencies and the energy difference $Ec_{15}-Ec_1$ between conduction band states.

III. APPLICATION TO ZINC TELLURIDE

We apply the theoretical description just presented by considering ZnTe which at $T=300$ K and below 9.5 GPa occurs in the zinc-blende crystal structure. Changes of Raman mode intensities under hydrostatic pressure have been reported recently.[11] The measurements for the TO(Γ) and LO(Γ) phonon lines were taken at room temperature in the backscattering configuration using diamond anvil cell (DAC) techniques. The experiment was not specifically designed for quantitative (relative) intensity measurements. These are difficult to perform in a DAC experiment because reflections at interfaces lead to admixtures of forward scattering if the sample is transparent for the exciting laser energy. However, the intensity changes for the TO and LO modes of ZnTe with increasing pressure were observed to be quite pronounced (see below). The observed pressure effects are assumed here to reflect the overall trends, at least at a semiquantitative level.

In order to evaluate the pressure dependence of $\partial S/\partial\Omega$ [Eq. (1)] and to compare with the experimental data it is necessary to consider the influence of pressure on all quantities appearing in Eqs. (9) and (15). The values of the quantities employed in our calculations are listed in Table I. For the refractive index an empirical expression was used, based on the Marple's equation[21] reported in Ref. 22. Reduced effective masses were evaluated in terms of the fundamental gaps according to the Kane model[22,23] and within the $\mathbf{k}\cdot\mathbf{p}$ theory. Thus, with the reduced masses μ, the following variations are obtained:

(i) Electron (Γ_{1c})–light hole (Γ_{15v})

$$\frac{m_0}{\mu_{lh}} = \frac{2P_0^2}{m_0E_g}\left[\frac{E_g+\frac{2}{3}\Delta}{E_g+\Delta}+\frac{2}{3}\right], \quad (18)$$

TABLE I. Values of parameters used for the calculation of the Raman intensities of ZnTe under pressure as plotted in Fig. 2. Pressure P is in GPa.

Parameter	Value
E_g	$(2.27+10.4\times10^{-2}P-28\times10^{-4}P^2)$ eV[a]
ω_{TO}	$(176.9+5.82P-0.13P^2)$ cm^{-1} [b]
ω_{LO}	$(206.1+4.74P-0.12P^2)$ cm^{-1} [b]
a_0	$(6.1037-0.391P-1.05\times10^{-3}P^2)$ Å[b]
μ_{lh}/m_0	$(0.0762+3.33\times10^{-3}P)$[c]
μ_{hh}/m_0	$(0.0918+2.57\times10^{-3}P)$[d]
μ_{0l}/m_0	$(0.0705-2.30\times10^{-4}P)$[e]
μ_{0h}/m_0	$(0.0832-1.7\times10^{-3}P)$[f]
$\delta=Ec_{15}-Ec_1$	$(3.2698-0.1148P+2.36\times10^{-3}P^2)$ eV
P^2/m_0	9.5 eV[g]
Q^2/m_0	15.5 eV[h]
Δ	0.96 eV[i]
ε_∞	7.4[g]
γ_1	3.8[j]
γ_2	0.72[j]
d_0	28 eV[k]

[a]Reference 33.
[b]Reference 11.
[c]See Eq. (18).
[d]See Eq. (19).
[e]See Eq. (20).
[f]See Eq. (21).
[g]Reference 22.
[h]Reference 34.
[i]Reference 24.
[j]Reference 35.
[k]Reference 12.

(ii) Electron (Γ_{1c})–heavy hole (Γ_{15v})

$$\frac{m_0}{\mu_{hh}} = 1+\frac{2P_0^2}{m_0E_g}\frac{E_g+\frac{2}{3}\Delta}{E_g+\Delta}+\gamma_1-2\gamma_2, \quad (19)$$

(iii) electron (Γ_{15c})–light hole (Γ_{15v})

$$\frac{m_0}{\mu_{0l}} = \frac{4}{3m_0}\left[\frac{P_0^2}{E_g}+\frac{Q^2}{Ec_{15}}\right]+\frac{2}{m_0}\frac{P'^2}{(Ec_{15}-Ec_1)}, \quad (20)$$

(iv) electron (Γ_{15c})–heavy hole (Γ_{15v})

$$\frac{m_0}{\mu_{0h}} = 1+\frac{4}{3m_0}\frac{Q^2}{Ec_{15}}+\frac{2}{3m_0}\frac{P'^2}{(Ec_{15}-Ec_1)}+\gamma_1-2\gamma_2. \quad (21)$$

Here γ_1 and γ_2 are the Luttinger parameters and Δ is the spin-orbit splitting, all three pressure independent.[24] In Table I we also quote the pressure dependence of μ_{lh}, μ_{hh}, μ_{0l}, and μ_{0h}.

As for the energy difference between the Γ_{1c} and Γ_{15c} gap energies, $\delta=Ec_{15}-Ec_1$ and its behavior under pressure P, we calculate the one-electron energies $E_n(\mathbf{k})$ for the bands $n=c_{15}$ and c_1 by employing the pseudopotential–plane-wave

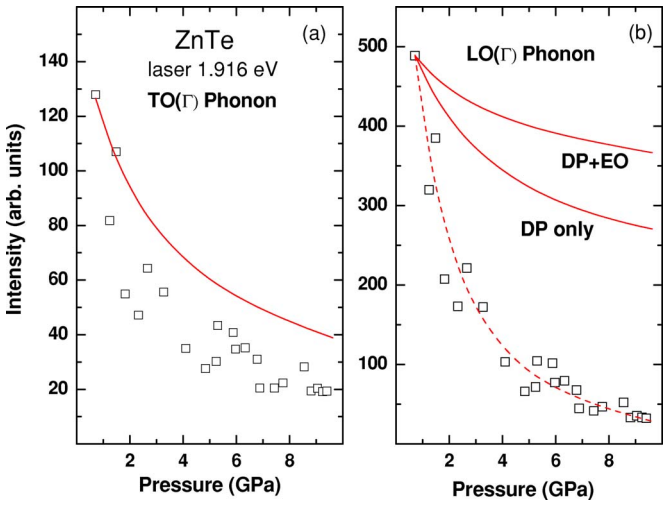

FIG. 2. (Color online) Integrated Raman intensities of the (a) TO(Γ) and (b) LO(Γ) phonon peak in ZnTe as a function of pressure. The solid line in (a) represents calculations according to Eqs. (1) and (9) with a background constant $A'=0$. In (b) solid lines correspond to calculations taking into account the deformation potential interaction only [Eq. (9)] and with the electro-optical contribution included [Eq. (15)]. Open squares are experimental data taken from Ref. 11. The dashed line in (b) is a fit according to Eq. (15) with a dispersionless background constant, independent of the pressure, A' equal to $1.34\times A^{DP}$ $(P=0)$. Calculated intensities are arbitrary and have been adjusted to overlap with the ranges used to represent experimental data.

method within the local-density approximation (LDA) to the density functional theory (DFT). It is well known that this approach cannot supply reliable values of the band gaps, nevertheless it has been shown[25] that it provides correct predictions for the *pressure variation* of the gaps. We used the VASP implementation[26–29] of the DFT, and the Vanderbilt-type pseudopotentials[30] as supplied by Kresse and Hafner.[31] The pseudopotential that we chose for Zn treats the semicore states explicitly, i.e., Zn is represented with 12 valence electrons $3d^{10}4s^2$, and the nonlinear core correction[32] has been applied as well. The calculations are carried out with the plane-wave cutoff energy of 19.3 Ry and the Brillouin zone sampling is based on the Γ-centered uniform mesh $8\times8\times8$. The calculated equilibrium corresponds to a lattice constant of $a_0=6.104$Å, $B_0=48$ GPa, $B_0'=4.7$ (Murnaghan equation of state), and the subsequent determination of the pressure coefficients was based on calculations of the one-electron energies $E_n(\vec{k})$ for $a_0=5.9$, 5.95, 6.0, 6.05, and 6.1 Å (a quadratic fit of the volume dependence). The obtained variation of $\delta=Ec_{15}-Ec_1$ with pressure is given in Table I and illustrated schematically in Fig. 1. Note that in ZnTe the energy separation decreases with increasing pressure.

In order to evaluate the optical deformation potential d_0 for the energy difference ΔE between the HH and LH valence bands at Γ we treated in the same fashion a structure with the frozen phonon TO(Γ), i.e., imposed displacements $\mathbf{u}(\mathrm{Te})=u(1,1,1)$ and $\mathbf{u}(\mathrm{Zn})=-u(1,1,1)M_{\mathrm{Te}}/M_{\mathrm{Zn}}$, with $u/a_0=\pm0.002$ and ±0.006 (i.e., four additional calculations). A weak nonlinearity in the $\Delta E(u)$ was eliminated by fitting the u dependence by a quadratic polynomial in u, and the pressure variation of the linear coefficient (i.e., of the deformation potential) was obtained by repeating the above calculations with lattice constants $a_0=6.10$, 6.01, 5.92, and 5.83 Å. We found that the variation of the deformation potential d_0 between 0 and 9.5 GPa is smaller than 0.5 eV. Thus, d_0 can be considered independent of pressure, and we used in the present calculations the experimental value given in Table I.

Figure 2(a) shows the integrated TO(Γ) intensity (open squares) for ZnTe measured as a function of the applied pressure [11] and using the excitation energy of $\hbar\omega_L=1.916$ eV, i.e., below the fundamental gap. The data can be compared with a calculation of the Raman intensity performed within the framework of the present model [Eqs. (1) and (9)] which is given by a solid line. In the calculation, the background constant A' was set equal to zero. Better agreement with the experiment could be forced if A' were fitted to the measured points. Such a procedure was used in several previous investigations of related problems under ambient-pressure conditions.[12,13,18]

Results for the Raman intensity of the LO(Γ) phonon are displayed in Fig. 2(b). The solid lines refer to the variation given by Eq. (9), i.e., corresponding to the DP interaction alone, and to the calculated intensity with the electro-optical contribution included [Eq. (15)]. Due to the decrease of the gap difference $\delta=Ec_{15}-Ec_1$ in the denominator of Eq. (17) the effective electro-optical constant $\alpha(P)$ increases with increasing pressure. As the pressure reduces the energy difference between the Γ_{15c} and Γ_{1c} states (see Table I) the interband Fröhlich interaction becomes stronger. Hence, if added to the deformation potential contribution with a negative sign, the EO contribution would reduce the total scattering intensity as a function of the pressure. In the calculation presented in Fig. 2(b) we chose the same sign for the DP and EO interactions, i.e., the same choice as the one reported for several II-VI semiconductors.[20]

The dashed line in Fig. 2(b) refers to a calculation according to Eq. (15) where the dispersionless background constant A' is chosen equal to $1.34\times A^{DP}$ $(P=0)$, so as to match the experimental data at $P=9.34$ GPa.

The main result of the theory outlined in Sec. II is that in ZnTe the integrated Raman intensity of the TO(Γ) and LO(Γ) modes decreases as the applied pressure increases. The most important factors controlling this variation are the dependence of the deformation potential scattering intensity on the electronic transitions and the variation of the phonon frequencies with pressure; in short form this can be written as

$$\frac{\partial S}{\partial\Omega}\propto\frac{N_0(P)+1}{[E_g(P)-\hbar\,\omega_S]\hbar\,\omega_{TO(LO)}(P)}. \tag{22}$$

The intensity is decreasing because, at higher values of the hydrostatic pressure, the E_g gap increases and so do the optical phonon energies $\hbar\omega_{TO}$ and $\hbar\omega_{LO}$. Other quantities involved in the DP process, such as the relative values of the effective masses, refractive index, or lattice constant, are smooth and slowly varying functions of P.

IV. CONCLUSIONS

We have examined theoretical expressions that determine the first-order Raman scattering intensities of a zinc-blende-type semiconductor as a function of applied pressure assuming the incoming laser energy is smaller than the fundamental gap. In zinc-blende semiconductors both the lowest direct gap E_g and the zone-center optical phonon frequencies at Γ increase with hydrostatic pressure. So, according to Eq. (22), the model predicts an overall decrease of the integrated Raman intensity of TO and LO modes with increasing pressure. We have introduced an effective electro-optical constant $\alpha(P)$ [Eq. (17)] that describes the pressure-dependent electro-optical contribution to the scattering probability amplitude of the LO(Γ) phonon. We conclude that in ZnTe the electro-optical interaction becomes increasingly important with increasing pressure for describing the LO scattering intensity relative to the TO scattering. It is believed that the microscopic phenomenological model employed here contains all essential mechanisms. Its application to pressure-dependent Raman scattering intensities of other semiconductors can be envisioned. A complementary approach would be to extend the *first-principles* density functional perturbation theory of Raman efficiencies [36] to the pressure dependence of Raman intensities in II-VI semiconductors.

ACKNOWLEDGMENTS

We acknowledge constructive comments by M. Cardona and R. Zeyher. C.T-G. is grateful to the Alexander von Humboldt Foundation and the Max-Planck Society for financial support and acknowledges the hospitality enjoyed during his stay at the Max-Planck-Institut für Festkörperforschung.

*Permanent address: Dept. of Theoretical Physics, Havana University, Vedado 10400, Havana, Cuba.

†Permanent address: Institut des Nanosciences de Paris, CNRS and Université Pierre and Marie Curie, 140 rue de Lourmel, F-75015 Paris, France.

[1] B. A. Weinstein and R. Zallen, in *Light Scattering in Solids IV*, edited by M. Cardona and G. Güntherodt, Topics in Applied Physics, Vol. 54 (Springer, Berlin, 1984), p. 463.

[2] E. Anastassakis and M. Cardona, in *High Pressure in Semiconductors Physics II*, edited by T. Suski and W. Paul, Semiconductors and Semimetals, Vol. 55 (Academic, New York, 1998), p. 118.

[3] M. Cardona, High Press. Res. **24**, 17 (2004).

[4] M. Cardona, Phys. Status Solidi B **241**, 3128 (2004).

[5] Richard M. Martin, Phys. Rev. B **4**, 3676 (1971).

[6] A. K. Sood, W. Kauschke, J. Menéndez, and M. Cardona, Phys. Rev. B **35**, 2886 (1987).

[7] W. Kauschke, N. Mestres, and M. Cardona, Phys. Rev. B **36**, 7469 (1987).

[8] A. Ingale, M. L. Bansal, and A. P. Roy, Phys. Rev. B **40**, 12353 (1989).

[9] A. Cantarero, C. Trallero-Giner, and M. Cardona, Phys. Rev. B **39**, 8388 (1989).

[10] C. Trallero-Giner, A. Cantarero, and M. Cardona, Phys. Rev. B, **40**, 4030 (1989).

[11] J. Camacho, I. Loa, A. Cantarero, and K. Syassen, J. Phys.: Condens. Matter **14**, 739 (2002).

[12] R. L. Schmidt, B. D. McCombe, and M. Cardona, Phys. Rev. B **11**, 746 (1975).

[13] M. Cardona, in *Light Scattering in Solids II*, edited by M. Cardona and G. Güntherodt, Topics in Applied Physics, Vol. 50 (Springer, Berlin, 1982), p. 19.

[14] A. Alexandrou, C. Trallero-Giner, G. Kanellis, and M. Cardona, Phys. Rev. B **40**, 1013 (1989).

[15] G. L. Bir and G. E. Pikus, *Symmetry and Strain-Induced Effects in Semiconductors* (Wiley, New York, 1974).

[16] P. Y. Yu and M. Cardona, *Fundamentals of Semiconductors* (Springer, Berlin, 2003).

[17] W. L. Faust and C. H. Henry, Phys. Rev. Lett. **17**, 1265 (1966).

[18] M. Rösch, R. Atzmüller, G. Schaack, and C. R. Becker, Phys. Rev. B **49**, 13460 (1994); see their Eq. (13).

[19] W. Richter, in *Solid State Physics*, edited by G. Höhler, Springer Tracts in Modern Physics, Vol. 78 (Springer, Berlin, 1976), p. 121.

[20] J. M. Calleja, H. Vogt, and M. Cardona, Philos. Mag. A **45**, 239 (1982).

[21] D. T. F. Marple, J. Appl. Phys. **69**, 539 (1964).

[22] M. Lindner, G. F. Schötz, P. Link, H. P. Wagner, W. Kuhn, and W. Gebhardt, J. Phys.: Condens. Matter **4**, 6401 (1992). Note two misprints in the sign of the fit parameters, the coefficients B and C. The correct expressions are $B=1.8+0.14P$ and $C=0.182-1.8\times10^{-2}P+1.08\times10^{-3}P^2$, with P in GPa.

[23] E. O. Kane, J. Phys. Chem. Solids **1**, 249 (1957).

[24] A. D. Brothers and J. B. Brungardt, Phys. Status Solidi B **99**, 291 (1980).

[25] K. J. Chang, S. Froyen, and M. L. Cohen, Solid State Commun. **50**, 105 (1984).

[26] G. Kresse and J. Hafner, Phys. Rev. B **47**, R558 (1993).

[27] G. Kresse, Ph.D. thesis, Technische Universität Wien, 1993.

[28] G. Kresse and J. Furthmüller, Comput. Mater. Sci. **6**, 15 (1996).

[29] G. Kresse and J. Furthmüller, Phys. Rev. B **54**, 11169 (1996).

[30] D. Vanderbilt, Phys. Rev. B **41**, 7892 (1990).

[31] G. Kresse and J. Hafner, J. Phys.: Condens. Matter **6**, 8245 (1994).

[32] S. G. Louie, S. Froyen, and M. L. Cohen, Phys. Rev. B **26**, 1738 (1982).

[33] K. Strössner, S. Ves, C. K. Kim, and M. Cardona, Solid State Commun. **61**, 275 (1987).

[34] M. Cardona, J. Phys. Chem. Solids **24**, 1543 (1963).

[35] H. P. Wagner, S. Lankes, K. Wolf, D. Lichtenberger, W. Kuhn, P. Link, and W. Gebhardt, J. Lumin. **52**, 41 (1992).

[36] M. Veithen, X. Gonze, and Ph. Ghosez, Phys. Rev. B **71**, 125107 (2005).